optics

MDPI

Article

Toraldo's Composed Pupil: A Theoretical Analysis of the Near Field

Daniela Mugnai [1,*], Pietro Bolli [2], Laura Burzagli [1] and Luca Olmi [2]

[1] Istituto di Fisica Applicata "Nello Carrara", CNR Area Della Ricerca di Firenze, Via Madonna del Piano 10, 50019 Sesto Fiorentino, Italy; l.burzagli@ifac.cnr.it
[2] Istituto Nazionale di Astrofisica (INAF), Osservatorio Astrofisico di Arcetri, Largo E. Fermi 5, 50125 Florence, Italy; pietro.bolli@inaf.it (P.B.); luca.olmi@inaf.it (L.O.)
* Correspondence: d.mugnai@ifac.cnr.it

Abstract: Over the years, there has been much speculation to understand whether (and how) it was possible to go below the diffraction limit. An advance in knowledge was achieved with the development of microwave techniques. In fact, more than fifty years after the publication of Toraldo's article dealing with this topic, some experimental measurements in the range of microwaves confirmed the validity of his model. Since some measurements were performed in the region of near field, while Toraldo's model refers to the far field, the need for a theoretical analysis in the framework of the Fresnel optics arose. The main goal of the present paper is to describe the problem of propagation in the near field (Fresnel optics) by using the same theoretical model already proposed by Toraldo. In order to test the validity of this new approach, the theoretical model has been compared with the FEKO simulation. The comparison of the theoretical model with the FEKO simulation in the far field for an open pupil (an open circular aperture) shows perfect agreement, as expected. We will demonstrate that there is also good agreement in the near field, although it is limited to the region around the main lobe, which is usually the region of main physical interest. Moving away from the main lobe, namely away from the optical axis, the agreement becomes less significant.

Keywords: super-resolution; near field; composed pupil

Citation: Mugnai, D.; Bolli, P.; Burzagli, L.; Olmi, L. Toraldo's Composed Pupil: A Theoretical Analysis of the Near Field. *Optics* **2024**, *5*, 319–329. https://doi.org/10.3390/opt5030023

Academic Editor: Thomas Seeger

Received: 19 April 2024
Revised: 17 June 2024
Accepted: 27 June 2024
Published: 10 July 2024

1. Introduction

The topic of super-resolution is undoubtedly one of the main topics studied in the field of physics because of its implications in theoretical physics (related to Heisenberg's uncertainty principle), as well as its possible practical applications.

After the pioneering paper of Schelkunoff [1] (in which it was demonstrated that the radiation pattern of a linear end-fire array of a given number of elements can be narrowed by a factor of more than two by carefully selecting the phase distribution of the currents relative to the several elements), in 1952, Giuliano Toraldo di Francia presented a theoretical study in which he demonstrated the possibility to increase the resolving power of an optical instrument with the use of special types of pupils (composed by concentric circular coronae), provided that specific requirements of the phase and amplitude of the single corona were satisfied [2].

Overcoming the diffraction limit is one of the main challenges that physicists have faced over the last hundred years. There has been much discussion as to whether this limit could be exceeded or not, and it was common opinion that, like the uncertainty principle in quantum mechanics, the diffraction limit seemed to be absolutely unsurmountable.

For this reason, Toraldo's model could not be ignored and found its first experimental confirmation in the range of microwaves [3,4] in 2003 and 2004. More than ten years later, some experimental measurements were performed at a frequency of 20 GHz [5], namely still in the range of microwaves but at a frequency different with respect to that of Refs. [3,4]. The interest in the 20 GHz measurement stems from the fact that it belongs

to one of the most common wavebands used in radio astronomy [5]. As in the case of Refs. [3,4], measurements at 20 GHz also deal with the diffraction field of a composed pupil which a plane wave affects. Since those measures were performed in the near field and Toraldo's model refers to the far field (see Appendix A), the need to have a theoretical model able to interpret those results arose.

Many studies have been dedicated to the evaluation of the near field in different physical systems, from antenna array technology to sensing and communications technology in view of new sixth-generation (6G) networks [6,7], to the characterization of bright and dark foci in the diffraction field [8], and to topics more related to quantum mechanics such as, theoretical statistics for systems describing the near field for photon antibunching and entanglement [9]. The literature relating to near-field propagation is extremely rich as regards super-resolution in the construction of images [10–15]. However, as far as we know, very little can be found in the literature regarding the super-resolution effects of electromagnetic propagation in the range of microwaves.

In this paper, we present, in Section 2, a theoretical model in order to analyze the diffraction in the near field for an open pupil as well as for a composed one. Then, in Section 3, we compare the theoretical results with the FEKO simulation; in Section 4, we present our conclusions, and finally, in Appendix A, we report a brief description of Toraldo's model.

2. Theoretical Analysis

Let us consider a plane wave normally incident on an opaque diaphragm (theoretically of infinite dimensions) with a generic aperture $\mathcal{C}$ whose extension is much smaller than the size of the diaphragm (see Figure 1).

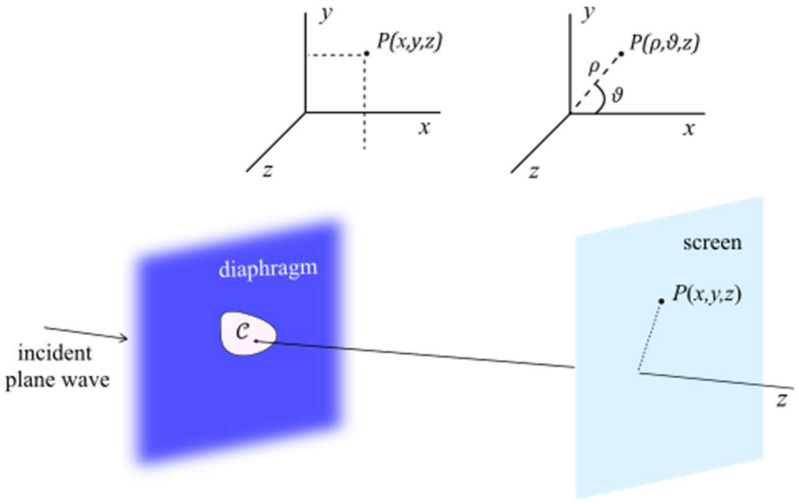

Figure 1. A schematic illustration of an electromagnetic diffraction process for a generic aperture $\mathcal{C}$. The field is detected over a screen positioned at a given distance from the diaphragm.

Under the condition that the distance between the diaphragm and the screen (or, more generally, the observation region) is much greater with respect to the dimension of the aperture $\mathcal{C}$, the diffracted field at a generic point $P(x, y, z)$ in the near region, and in the scalar approximation, can be written as [16]

$$E = \frac{A}{\lambda} \frac{\exp\left[i\left(kz - \frac{\pi}{2}\right)\right]}{z} \iint_{\mathcal{C}} \exp\left\{i\frac{k}{2z}\left[\left(x' - x\right)^2 + \left(y' - y\right)^2\right]\right\} dx'dy', \quad (1)$$

where λ is the wavelength, $k = 2\pi/\lambda$ is the wave number, A is the amplitude of the incident wave, and x' and y' are the Cartesian coordinates of a point over the diaphragm (Equation (1) can be generalized also for a diaphragm with more than one aperture by simply adding other integrals for additional apertures). We wish to recall that in the case of

a circular aperture, the near region can be defined as the region of radius $R \lesssim \left(2D^2\right)/\lambda$, where D is the diameter of the source and λ is the wavelength.

In the case in which the aperture is characterized by rotational symmetry, it is convenient to use polar coordinates. Let us denote with ρ' and θ' the coordinates of a point over the diaphragm, and with ρ and θ, the ones of a point on the screen, such as

$$\begin{array}{ll} x' = \rho' \cos\theta', & x = \rho\cos\theta \\ y' = \rho' \sin\theta', & y = \rho\sin\theta; \end{array} \tag{2}$$

therefore, we have the following:

$$\begin{gathered} (x'-x)^2 + (y'-y)^2 = \\ = \rho'^2 + \rho^2 - 2\rho\rho'\left(\cos\theta\cos\theta' + \sin\theta\sin\theta'\right) = \rho'^2 + \rho^2 - 2\rho\rho'\cos(\theta'-\theta)\Big). \end{gathered}$$

In Equation (1), we can change the integration variables from dx', dy' to $d\rho', d\theta'$ by using the Jacobian determinant, and we obtain

$$dx'\,dy' = \rho' d\rho' d\theta'.$$

By substituting previous equations into Equation (1), the diffraction field for a circular aperture becomes

$$E = \frac{A}{\lambda}\,\frac{\exp\left\{i\left[k\left(z+\frac{\rho^2}{2z}\right)-\frac{\pi}{2}\right]\right\}}{z}\int_0^{D/2}\exp\left(ik\frac{\rho'^2}{2z}\right)\rho' d\rho'\int_0^{2\pi}\exp\left[-ik\frac{\rho\rho'}{z}\cos(\theta'-\theta)\right]d\theta',$$

with D being the diameter of the aperture. By recalling the integral representation of the Bessel function of first kind, that is

$$J_n(\alpha) = \frac{(-i)^n}{\pi}\int_0^{\pi}\exp(i\alpha\cos\theta)\cos(n\theta)\,d\theta\,,$$

and by considering that the cosine function is an even function, we obtain

$$E = 2\pi\,\frac{A}{\lambda}\,\frac{\exp\left[i\left(kR-\frac{\pi}{2}\right)\right]}{z}\int_0^{D/2}\exp\left(ik\frac{\rho'^2}{2z}\right)J_0\left(k\frac{\rho\rho'}{z}\right)\rho' d\rho'\,, \tag{3}$$

where $R = z + \left(\rho^2/2z\right)$ (for $\rho \ll z$, R is approximately equal to the distance between the center of the diaphragm and a given point on the screen) and J_0 is the zero-order Bessel function of first kind.

Equation (3) can be integrated by parts by using the following well-known formula:

$$\int u\,dv = vu - \int v du\ ,$$

and by choosing

$$dv = \rho' J_0\left(k\frac{\rho\rho'}{z}\right)d\rho', \qquad u = \exp\left(ik\frac{\rho'^2}{2z}\right),$$

the integration of Equation (3) gives

$$\begin{gathered} E = 2\pi\,\tfrac{A}{\lambda}\,\tfrac{\exp\left[i\left(kR-\frac{\pi}{2}\right)\right]}{z}\left\{\left[\rho'\left(\tfrac{z}{k\rho}\right)J_1\left(k\tfrac{\rho\rho'}{z}\right)\,\exp\left(ik\tfrac{\rho'^2}{2z}\right)\right]_0^{\frac{D}{2}} - \right. \\ \left. -i\int_0^{D/2}\frac{\rho'^2}{\rho}\,J_1\left(k\tfrac{\rho\rho'}{z}\right)\exp\left(ik\tfrac{\rho'^2}{2z}\right)\,d\rho'\right\}. \end{gathered} \tag{4}$$

By evaluating the term in the square brackets, we obtain

$$E = A\left(\frac{D}{2\rho}\right)\exp\left[i\left(kR-\frac{\pi}{2}\right)\right]J_1\left(\pi\frac{\rho D}{\lambda z}\right)\exp\left(i\pi\frac{D^2}{4\lambda z}\right)- \\ -i\int_0^{D/2}\frac{\rho'^2}{\rho}\,J_1\left(k\frac{\rho\rho'}{z}\right)\exp\left(ik\frac{\rho'^2}{2z}\right)\,d\rho'. \tag{5}$$

We can now continue by solving the integral in Equation (5), still by using the integration by parts, whose solution gives rise to an integral which can be solved again by the integration by parts, and so on. Generally speaking, we can see that the solution of the integral like that of Equation (3) gives rise to a series of the type

$$\int_0^{\varepsilon}\exp\left(ia\phi^2\right)\,J_0(b\phi)\,\phi\,d\phi = \left(\frac{\varepsilon}{b}\right)\exp\left[ia\varepsilon^2\right]\times \\ \times\left[J_1(b\varepsilon)-i\left(2a\,\frac{\varepsilon}{b}\right)\,J_2(b\varepsilon)-\left(2a\,\frac{\varepsilon}{b}\right)^2J_3(b\varepsilon)+i\left(2a\,\frac{\varepsilon}{b}\right)^3+\cdots\right]. \tag{6}$$

In the present case, $a = k/2z, b = k\rho/z$, and $\varepsilon = D/2$; therefore, the final result is

$$E = A\left(\frac{D}{2\rho}\right)\exp\left[i\left(kR-\frac{\pi}{2}\right)\right]\exp\left(i\pi\frac{D^2}{4\lambda z}\right)\,\left[\,J_1\left(\pi\frac{\rho D}{\lambda z}\right)-i\left(\frac{D}{2\rho}\right)J_2\left(\pi\frac{\rho D}{\lambda z}\right)- \\ -\left(\frac{D}{2\rho}\right)^2J_3\left(\pi\frac{\rho D}{\lambda z}\right)+i\left(\frac{D}{2\rho}\right)^3J_4\left(\pi\frac{\rho D}{\lambda z}\right)+\left(\frac{D}{2\rho}\right)^4J_5\left(\pi\frac{\rho D}{\lambda z}\right)-\cdots\right]. \tag{7}$$

If we limit ourselves to the first term E_1 inside brackets in Equation (7), namely

$$E_1 = A\left(\frac{D}{2\rho}\right)\exp\left[i\left(kR-\frac{\pi}{2}\right)\right]\exp\left(i\pi\frac{D^2}{4\lambda z}\right)J_1\left(\pi\frac{\rho D}{\lambda z}\right), \tag{8}$$

we obtain an amplitude $|E_1|$ which has the same behavior as the far field A_{ff} (as expected), which can be written as (see Appendix A)

$$A_{ff} = \frac{A}{2\lambda\sin\theta}\left[DJ_1\left(\pi\frac{D}{\lambda}\sin\theta\right)\right] \simeq A\frac{zD}{2\lambda x}\,J_1\left(\pi\frac{Dx}{\lambda z}\right), \tag{9}$$

where $x \equiv \rho$, and where we have made the substitution $\sin\theta = x/\sqrt{x^2+z^2} \simeq x/z$ $(z \gg x)$.

This means that the near field is described by an equation in which the first term is similar to that of the far field (the only difference lies in the numerical factor), which is dominant for $z \gg D$, while the other terms constitute a correction that becomes more and more important when the value of z approaches D. The results are shown in Figure 2: in (a), we can see that the first term of Equation (7) (dotted line) is exactly equal to the value of the far field (solid line), while in (b), the total value of Equation (7) (dotted line) shows a clear discrepancy between the near and far field when z approaches D.

Once the diffracted field in the near field is known for a circular aperture, namely for an open pupil, it is easy to estimate the diffracted field for a circular corona which can be evaluated by the difference between the transmitted and the reflected fields. If we indicate with D_1 and D_2 the diameters of the internal and external circumferences, respectively (see Figure 3), then the diffracted amplitude A_c for the circular corona is given by (still for an incident plane wave)

$$A_c = |E(D_2) - E(D_1)|\ , \tag{10}$$

where E is given by Equation (7).

The material surrounding the pupil is assumed to be a perfect electric conductor (PEC), thus totally reflecting the electromagnetic radiation (blue color in Figure 3). In the microwave range, the material through which the field is transmitted (white color in Figure 3) is constituted, for instance, by a dielectric whose thickness is selected to produce the dephasing required by the theoretical model in order to obtain super-resolution.

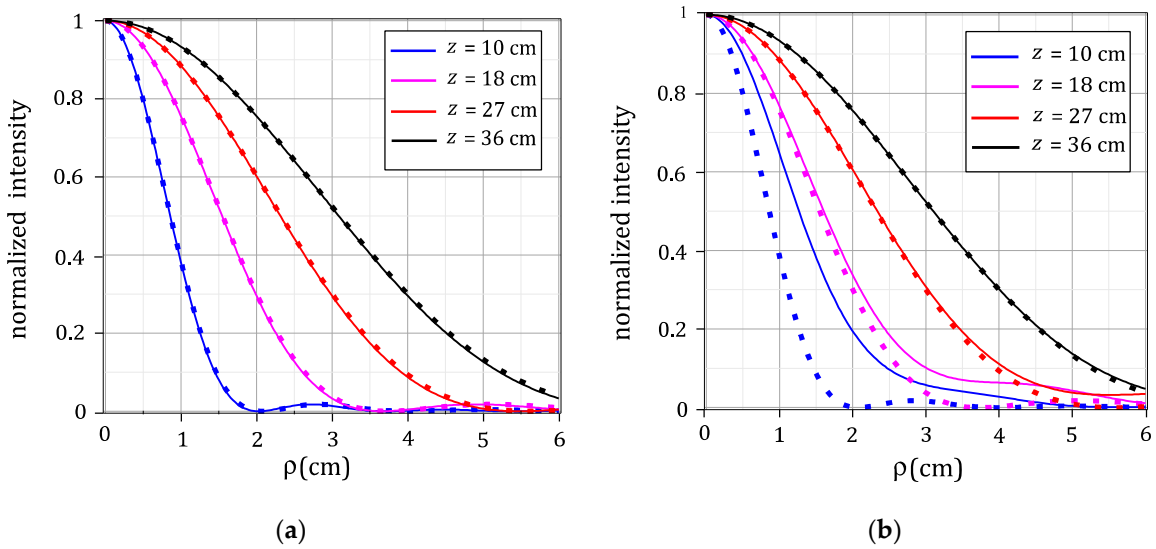

Figure 2. The normalized intensity at a point P on the screen as a function of the radial coordinate for diffraction by an open pupil (a circular aperture) and for different values of z, for $D = 9$ cm and $\lambda = 1.5$ cm. The dotted lines refer to the far field, while the solid lines refer to the near field evaluated by (**a**) the first term of Equation (7); (**b**) all of Equation (7) till the 7th term of the series. As expected, the first term of the series of (7), which refers to the near field, is equal to that of the far field (when normalized), while the total near field is equal to the far field only for values of z sufficiently greater than the diameter of the aperture. When the value of z approaches D, the discrepancy between the near and far field becomes more and more evident.

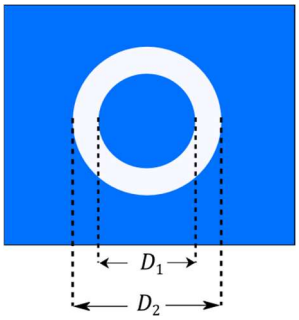

Figure 3. A drawing of a single corona whose external and internal diameters are D_2 and D_1, respectively.

The result of Equation (10) can be generalized for any system constituted by N circular coronae plus the open pupil in the center. By denoting with E_n the contribution of each corona, and by E_0 the contribution due to the central pupil (coincident with $E(D_2)$ in Equation (10)), the total diffracted amplitude A_t is given by

$$A_t = |E_0 \pm \sum_N E_n| \,, \tag{11}$$

where the plus sign refers to the transmitted field, and the negative one to the reflected field.

3. Theoretical Model and FEKO Simulation Results

In order to evaluate the reliability of the theoretical model, we can compare it with the results of the commercial software FEKO© [17], a comprehensive EM simulation software tool used for the electromagnetic field analysis of $3D$ structures.

Let us compare the normalized amplitude evaluated by the theoretical model, Equation (7), and by FEKO, for an open pupil of diameter $D = 9$ cm, at a frequency of 20 GHz, and for a distance $z = 18$ cm (Figure 4a). The choice of these values is due to the fact that some experimental measurements have been performed precisely for these values [5].

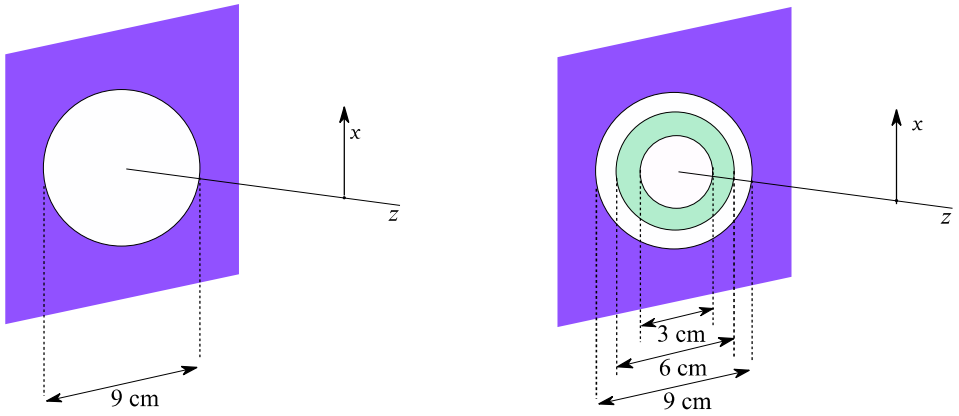

Figure 4. A drawing of an open pupil (**a**) and a system constituted by two coronae plus the central aperture (**b**).

As we can see in Figure 5, the results are in good agreement almost everywhere, showing only an opposition of the phase in the tail, around the value of 8 cm, i.e., very close to the edge of the pupil. This modest discrepancy may be due (apart from the different way to evaluate the field) to the fact that the value of z (=18 cm) cannot be considered much greater with respect to D (=9 cm), a condition required by the theoretical model described in the previous section.

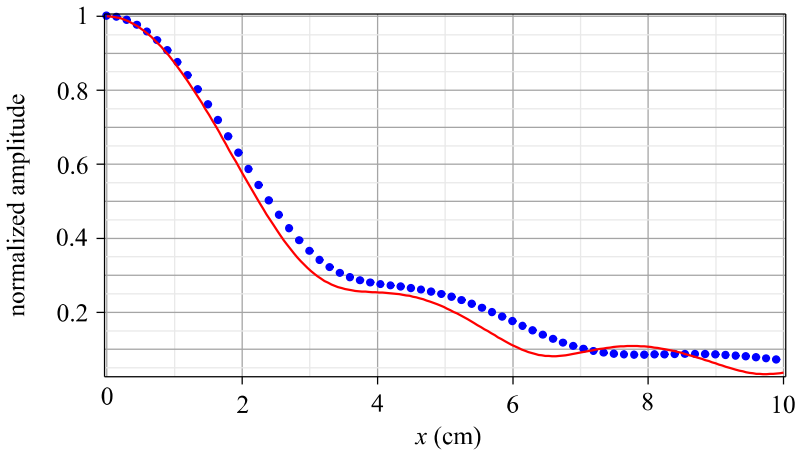

Figure 5. The normalized amplitude diffracted by an open pupil: the field is evaluated at $z = 18$ cm. Other parameter values are the same as in Figure 2. The solid red line is the theoretical model (Equation (7)), while the dotted line is the result obtained by the FEKO simulation.

As a further step, let us consider a composed pupil (hereafter named TP3) constituted by two coronae plus the central pupil, as shown in Figure 4b. In this case, if we denote with E_1 and E_2 the contribution of the transmitted and reflected fields by the external and internal coronae, respectively (each one evaluated through Equation (10)), and with E_0 the contribution due to the central pupil (Equation (7)), the total transmitted amplitude A_t can be written as

$$A_t = |E_0 + E_1 - E|. \tag{12}$$

As required by Toraldo's model, in order to have super-resolution, each corona must satisfy specific conditions for the phase and amplitude (see Appendix A). However, the condition of the phase alone is a necessary and sufficient condition in order to have super-resolution; thus, in the case of TP3, the previous condition is satisfied by adding a π factor to the phase of the innermost corona.

In Figure 6, we report the results of the theoretical model for a TP3 composed pupil together with the results of the FEKO simulation; we can see that both the TP3 theoretical model and the FEKO simulation clearly show a narrower main lobe compared to the open pupil. We can also see that there is rather good agreement between the theoretical model and FEKO simulation, especially in the region of physical interest, namely the main lobe. The discrepancy in the area beyond 6 cm may be due to the fact that, as previously discussed, Equation (7) has been obtained under the condition that the distance z is much greater with respect to the dimension of the aperture. Actually, it is not easy to establish when this condition is fully satisfied, and this may be the reason why there is not perfect agreement between the two approaches. Moreover, we have to recall that Toraldo's model in the near field is described by an infinite series, which cannot be totally evaluated, and the FEKO simulator is not able to reproduce the exact theoretical model presented here (we will discuss this issue in our conclusions).

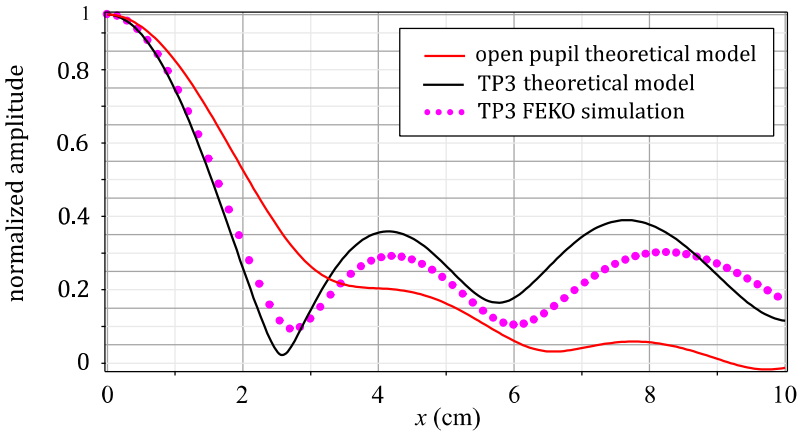

Figure 6. The normalized amplitude, as a function of the transversal coordinate §, evaluated by Equation (7) ($\rho \equiv x$, solid black line) and by the FEKO simulation (dotted magenta line). The dimension of the composed corona is the same as in Figure 4b. For comparison, the amplitude of the open pupil is also shown (solid red line). The parameter values are the same as in Figure 2.

In Figure 7, we show the diffraction amplitude for a TP4 pupil, i.e., composed of three coronae plus the central open aperture (Figure 7a), which again shows a narrower main lobe. The agreement between the theoretical model and the FEKO simulation is still good, except for x $\gtrsim$ 6 cm, where, except for a slight difference in the amplitude, there is a shift in the position of the maxima and minima.

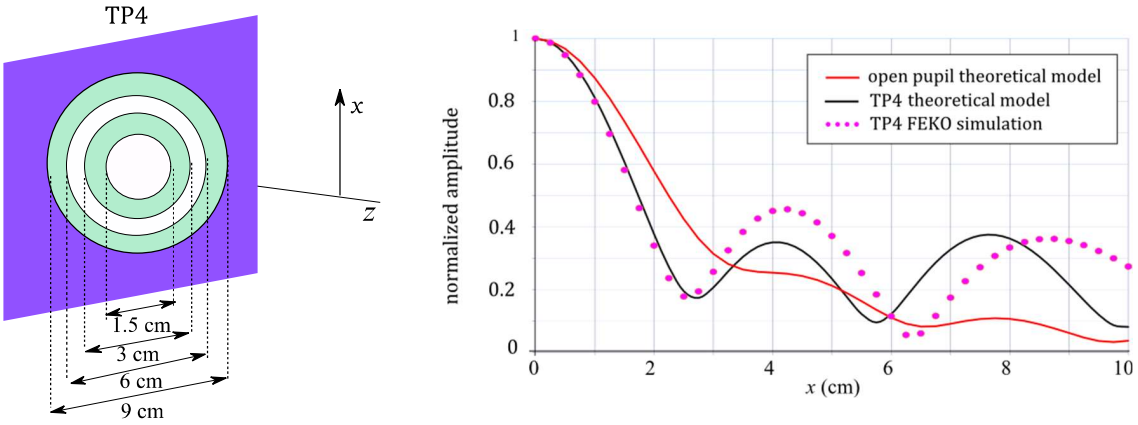

(**a**) (**b**)

Figure 7. Composed pupil TP4 (**a**) and relative diffraction amplitude (**b**). Symbols and parameter values are same as in Figure 6.

As a final test, we have also performed a comparison between the analytical model and the FEKO simulations in the case of a five-coronae TP (or TP5) in the far field (Figure 8). We note again reasonable agreement in the region of the main lobe, while the sidelobes appear quite different between the theoretical model and the numerical simulation. The possible reasons for this disagreement will be discussed in our conclusions.

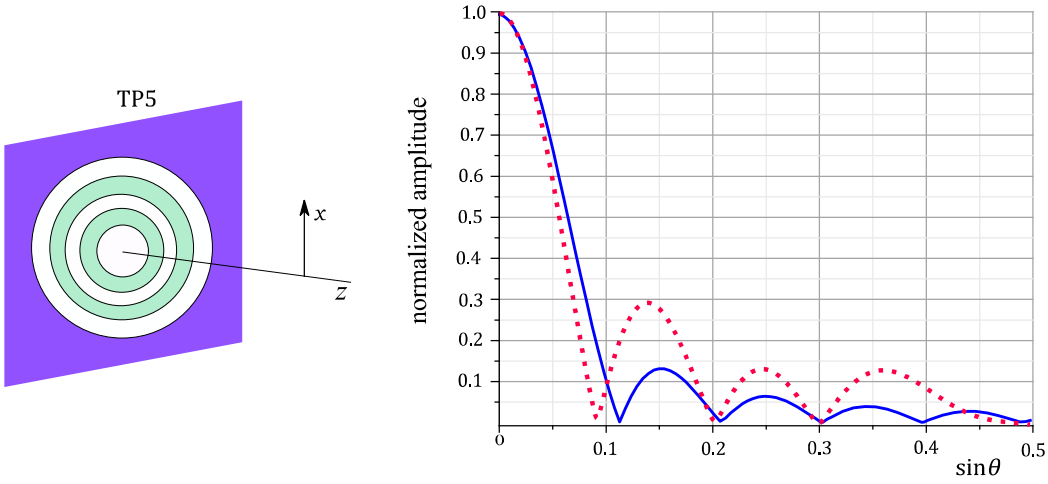

(**a**) (**b**)

Figure 8. (**a**) A composed TP5 pupil and (**b**) an evaluation of the relative amplitude in the far field (Fraunhofer region) as a function of the diffraction angle θ. The red dotted line represents the FEKO simulation, while the solid blue one is the result of the theoretical model evaluated by Equation (7) with z = 5000 cm. Starting from the central pupil, the diameters are 1.5, 3.6, 7.2, 9, and 16 cm.

As previously mentioned, simulations at 20 GHz were chosen because of its applications in radio astronomy. In fact, the work presented here is part of a larger project, named "Pupille Toraldo" (or PUTO for short), which is devoted to the designing, testing, and implementing of a super-resolution optical system on a radio telescope. As part of this project, and based on the theoretical model and our FEKO simulations, we conducted more comprehensive laboratory tests at the selected frequency of 20 GHz [5]. These tests clearly showed that the super-resolution effect was achieved and also showed good agreement with what was expected. After confirming the presence of super-resolving effects, we designed an optical module based on a two-lens collimator placed after the Cassegrain focus of the telescope and before the receiver dewar. The first lens of the collimator generates an image of the primary reflector which is then brought into a subsequent focus by the second lens. Toraldo's pupil is placed at the image of the entrance pupil where it can modify the incident wavefront [18].

After further tests (inside an anechoic chamber) of the two-lens collimator, which showed results quite consistent with the FEKO simulation, the Toraldo's pupil optical module was successively mounted on a small Cassegrain antenna 125 cm in diameter [19] with the same focal ratio ($\simeq$3) as the Medicina 32 m radio telescope [20]. Electromagnetic simulations and preliminary field tests of the antenna plus optical module have shown that super-resolution can be achieved with this optical arrangement. An improved Toraldo's pupil optical module is now being designed for applications with the Istituto Nazionale di Astrofisica (INAF) radio telescopes.

4. Conclusions

The concept of super-resolution refers to various methods for improving the angular resolution of an optical imaging system beyond the classical diffraction limit. Variable transmittance pupils constitute an attractive method to achieve super-resolution, and Toraldo's pupils represent the simplest example of such filters.

We have analyzed the field diffracted by Toraldo's pupils and found a formula for the complex amplitude in the near-field region. We have then compared our result with FEKO numerical simulations at 20 GHz for a few Toraldo's pupils. We found reasonable agreement between the FEKO results and our theoretical model, with some deviations outside the main lobe.

On the one hand, the theoretical model suffers some approximations and therefore has some limitations in the near field (but in the far field, it proved to work well). On the other hand, the FEKO simulator is not totally reliable because of difficulties in modeling complex systems such as those represented by Toraldo's pupils. More specifically, the FEKO solver is based on the full-wave technique of the Method of Moment, which solves Maxwell's equations numerically. Therefore, FEKO provides an exact solution of the EM problem, but with a finite accuracy determined by the selected meshing of the set-up geometry.

In the case under consideration, the diaphragm consists of a finite screen illuminated by an incident plane wave, therefore producing significant diffraction from the edges of the screen. This deviates from the theoretical model where external diffraction does not exist thanks to the assumption of an infinite screen. Using a directive horn antenna instead of a plane wave has been tested to reduce the illumination of the edges of the plane, but it caused a non-uniform phase in the diaphragm plane. Another difference between the theoretical model and FEKO is in the dielectric thickness, which is infinitesimal and finite in the two approaches, respectively. Finally, in the FEKO model, the electric field transported by the EM wave features two orthogonal components, namely the main component (co-polar) and the unwanted component (cross-polar), while in the theoretical model, the latter component is neglected.

Therefore, the theoretical model results and the FEKO results are expected to show some discrepancies, although both approaches are able to describe quite well the propagation in the case of Toraldo's pupils. For an ideal system (namely infinite screen, an ideal incident plane wave, zero thickness for materials composing pupils, etc.), the theoretical model is probably more reliable. On the contrary, for a real system, in which previous conditions are not satisfied, FEKO simulation represents the better tool to be utilized.

The convenience of the theoretical model is that it can be used to predict the profile of the near field generated by Toraldo's pupil in order to select the best geometry for a specific application. For optical systems more complex compared to the simple Toraldo's pupil, the theoretical model can be useful for speeding up the optimization procedure, which is not always easy to implement and often takes a long time with electromagnetic software tools.

Author Contributions: Conceptualization, D.M.; software, P.B.; formal analysis, D.M. and L.O.; resources, L.B.; writing—original draft preparation, D.M.; writing—review and editing, D.M., L.O., P.B. and L.B. All authors have read and agreed to the published version of the manuscript.

Funding: This research received no external funding.

Data Availability Statement: No new data are available.

Conflicts of Interest: The authors declare no conflict of interest.

Appendix A

Toraldo's model [2] for the evaluation of the diffraction amplitude due to a plane wave incident on a composed pupil, which consists of concentric circular slits, can be summarized as follows.

In the far field, the amplitude $A_{ff}(\theta)$ diffracted by an open pupil (still for an incident plane wave) can be written as

$$A_{ff}(\theta) = \frac{A}{2\lambda \sin\theta} \left[D J_1 \left(\pi \frac{D}{\lambda} \sin\theta \right) \right], \tag{A1}$$

where θ is the diffraction angle, D is the diameter of the pupil, λ is the wavelength, and J_1 is the first-order Bessel function of first kind. The normalized square of the amplitude of the previous equation is exactly equal to the Airy disk.

Starting from Equation (A1), it is easy to obtain the diffraction pattern for a circular corona, which is simply given by the difference between the amplitude of the corona of the major diameter D_2 and that of the lower diameter D_1 (which gives only the reflected field):

$$A_{ff}(\theta) = \frac{A}{2\lambda \sin\theta}\left[D_2 J_1\left(\pi\frac{D}{\lambda}\sin\theta\right) - D_1 J_1\left(\pi\frac{D}{\lambda}\sin\theta\right)\right]. \tag{A2}$$

By generalizing the results of Equation (A2) to a system constituted by n circular coronae, we can write

$$A_{ff}(x) = \sum_{i=0}^{n-1}\frac{\gamma_{i+1}}{x}\left[\alpha_{i+1}J_1\left(\alpha_{i+1}x\right) - \alpha_i J_1\left(\alpha_i x\right)\right], \tag{A3}$$

where $x = \pi\left(\frac{D}{\lambda}\right)\sin\theta$, $\alpha_i = D_i/D_{\max}$ is the ratio between a given diameter and the maximum diameter, and

$$\gamma_{i+1} = \frac{\pi D^2}{2\lambda^2}A_{i+1}$$

is a constant that is proportional to the amplitude A_{i+1} illuminating each corona. For a given pupil divided into a given number of n coronae, we can impose in Equation (A3) n independent conditions—for instance, the x values of its zeros—thus obtaining a system of n equations from which we can determine the n coefficients $\gamma_1 \cdots \gamma_n$. The values of the coefficients $\gamma_1 \cdots \gamma_n$, when substituting them into Equation (A3), will allow us to know the values of the phase and the amplitude to be chosen in order to obtain the diffraction behavior we want.

References

1. Schelkunoff, S.A. A Mathematical Theory of Linear Arrays. *Bell Syst. Tech. J.* **1943**, *22*, 80–107. [CrossRef]
2. Toraldo di Francia, G. Super-gain antennas and optical resolving power. *Nuovo Cimento Suppl.* **1952**, *9*, 426–438. [CrossRef]
3. Mugnai, D.; Ranfagni, A.; Ruggeri, R. Pupils with super-resolution. *Phys. Lett. A* **2003**, *311*, 77–81. [CrossRef]
4. Ranfagni, A.; Mugnai, D.; Ruggeri, R. Beyond the diffraction limit: Super-resolving pupils. *J. Appl. Phys.* **2004**, *95*, 2217–2222. [CrossRef]
5. Olmi, L.; Bolli, P.; Cresci, L.; D'Agostino, F.; Migliozzi, M.; Mugnai, D.; Natale, E.; Nesti, R.; Panella, D.; Stefani, L. Laboratory measurements of super-resolving Toraldo pupils for radio astronomical applications. *Exp. Astron.* **2017**, *43*, 285–309. [CrossRef]
6. Liu, Y.; Wang, Z.; Xu, J.; Ouyang, C.; Mu, X.; Schober, R. Near-Field Communications: A Tutorial Review. *IEEE Open J. Commun. Soc.* **2023**, *4*, 1999–2049. [CrossRef]
7. Wang, Z.; Mu, X.; Liu, Y. Near-field integrated sensing and communications. *IEEE Commun. Lett.* **2023**, *27*, 2048–2052. [CrossRef]
8. Rodrigues Gonçalves, M.; Rozenman, G.G.; Zimmermann, M.; Efremov, M.A.; Case, W.B.; Arie, A.; Shemer, L.; Schleich, W.P. Bright and dark diffractive focusing. *Appl. Phys. B* **2022**, *128*, 51. [CrossRef]
9. Bello, F.; Kongsuwan, N.; Donegan, J.F.; Hess, O. Controlled cavity-free, dingle-photon emission and bipartite entanglement of near-field-excited quantum emitters. *Nano Lett.* **2020**, *20*, 5830–5836. [CrossRef] [PubMed]
10. Qu, J.; Yang, Z. (Eds.) *Super Resolution Optical Imaging and Microscopy: Methods, Algorithms, and Applications*; Wiley: Weinheim, Germany, 2024.
11. Gramotnev, D.K.; Bozhevolnyi, S.I. Plasmonics beyond the diffraction limit. *Nat. Photonics* **2010**, *4*, 83–91. [CrossRef]
12. Shahram, M.; Milanfar, P. Imaging below the diffraction limit: A statistical analysis. *IEEE Trans. Image Process.* **2004**, *13*, 677–689. [CrossRef] [PubMed]
13. Grosjean, T.; Courjon, D.; Van Labeke, D. Bessel beams as virtual tips for near-field optics. *J. Microsc.* **2003**, *210*, 319–323. [CrossRef] [PubMed]
14. Vigoureux, J.M.; Courjon, D. Detection of nonradiative fields in light of the Heisenberg uncertainty principle and the Rayleigh criterion. *Appl. Opt.* **1992**, *31*, 3170–3177. [CrossRef] [PubMed]
15. Sheppard, C.J.R. Resolution and super-resolution. *Microsc. Res. Tech.* **2017**, *80*, 590–598. [CrossRef] [PubMed]
16. Di Francia, G.T. I fenomeni di Fresnel—Chapter XI. In *La Diffrazione della Luce*; Edizioni Scientifiche Einaudi; Boringhieri Pub.: Torino, Italy, 1953.
17. ALTAIR. Available online: https://altairhyperworks.com/product/FEKO (accessed on 30 October 2023).

18. Olmi, L.; Bolli, P.; Carbonaro, L.; Cresci, L.; Mugnai, D.; Natale, E.; Nesti, R.; Panella, D.; Roda, J.; Zacchiroli, G. Design of super-resolving Toraldo Pupils for radio astronomical applications. In Proceedings of the XXXIInd General Assembly and Scientific Symposium of the International Union of Radio Science (URSI GASS), Montreal, QC, Canada, 19–26 August 2017; pp. 1–4.
19. Available online: https://sites.google.com/inaf.it/arcetriradiogroup/research-activities#h.5vm5xicaih5l (accessed on 6 March 2024).
20. Olmi, L.; Bolli, P.; Carbonaro, L.; Cresci, L.; Donati, A.; Marongiu, P.; Mugnai, D.; Natale, E.; Nesti, R.; Panella, D. Simulations and Tests of a Super-Resolving Optical Module Using a Satellite Antenna. In Proceedings of the 23rd International Conference on Applied Electromagnetics and Communications (ICECOM), Dubrovnik, Croatia, 30 September–2 October 2019; pp. 1–4.